Fiber Tract Mapping from Diffusion Tensor MRI *

B. C. Vemuri[1] Y. Chen[2] M. Rao[2] T. McGraw[1], Z. Wang[1] T. Mareci[3]
[1]Dept. of CISE [2]Dept. of Mathematics [3]Dept. of Biochemistry
University of Florida
Gainesville, Fl. 32611

UF-CISE TR01-004

Abstract

To understand evolving pathology in the central nervous system (CNS) and develop effective treatments, it is essential to correlate the nerve fiber connectivity with the visualization of function. Such information is fundamental in CNS processes since anatomical connections determine where information is passed and processed. Diffusion tensor imaging (DTI) can provide the fundamental information required for viewing structural connectivity. However, robust and accurate acquisition and processing algorithms are needed to accurately map the nerve connectivity. In this paper, we present a novel, algorithm for automatic fiber tract mapping in the CNS specifically, the spinal cord. The automatic fiber tract mapping problem will be solved in two phases, namely a data smoothing phase and a fiber tract mapping phase. In the former, smoothing is achieved via a new weighted TV-norm minimization which strives to smooth while retaining all relevant detail. Existence and uniqueness results for this minimization are presented in brief. For the fiber tract mapping, a smooth 3D vector field indicating the dominant anisotropic direction at each spatial location is computed from the smoothed data. Fiber tracts are then determined as the smooth integral curves of this vector field in a variational framework. To facilitate visualization of the computed fiber tracts, we overlay the 3D fibers on a volume rendering of the DT-MR scan. Examples are presented for DT-MR data sets from a normal and injured rat spinal cords respectively.

1 Introduction

Fundamental advances in understanding living biological systems require detailed knowledge of structural and functional organization. This is particularly important in the nervous system where anatomical connections determine the information pathways and how this information is processed. Our current understanding of the nervous system is incomplete because of a lack of fundamental structural information [13] necessary to understand function. For the entire central nervous system, understanding and treating evolving pathology, such as spinal cord injury, depends on a detailed understanding of the anatomical connectivity changes and how they relate to function. For example, an evolving spinal cord lesion undergoes an initial response to an insult which is followed by a sequence of secondary events leading to further tissue degradation [37]. A method for defining the structure-function relationship is needed that can be used in the whole living organism that facilitates the study of such an evolving dynamics process.

Recently MR imaging has been used to study the structural connectivity within whole living organisms. The MR measurement of water translational self-diffusion provides a method that can be used to study structural connectivity with ubiquitous indigenous material, water. In highly organized nervous tissue, like white matter, diffusion anisotropy can be used to visualize fiber tracts. Douek, et al. [14] have used diffusion measurements along three orthogonal axes to estimate diffusion anisotropy in human brain white matter. From this data, they produced a color map of the fiber orientations reflective of white matter organization. Recently MR measurements have been developed to measure the tensor of diffusion. This provides a complete characterization of the restricted motion of water through the tissue that can be used to infer tissue structure and hence fiber tracts. The development of diffusion tensor acquisition, processing, and analysis methods provides the framework for creating fiber tract maps based on this complete diffusion tensor analysis [12, 17, 19, 21].

For automated fiber tract mapping, prior to estimating the diffusion tensor, the raw data must be smoothed while preserving relevant detail. The raw data in this context consists of seven directional images acquired for varying magnetic field strengths. Note that atleast seven values at each 3D grid point in the data domain are required to estimate

*This research was in part funded by the NSF grant IIS-9811042 and NIH RO1-RR13197

the six unknowns in the symmetric 2-tensor and one scale parameter. The data smoothing or de-noising can be formulated using variational principles which in turn require solutions to PDEs. Recently, there has been a flurry of activity on the PDE-based smoothing schemes. In [25], Perona and Malik developed an *anisotropic diffusion* scheme for image smoothing. The basic idea of this nonlinear smoothing scheme was to smooth the image while preserving the edges in it. This was done by using the following equation $I_t = div(c(\nabla I)\nabla I)$, where I is the image to be smoothed and I_t describes its evolution over time, and $c(\nabla I)$ is a decreasing function of ∇I. Catte et al., [5], Nitzberg and Mumford [22] and Alvarez *et al.* [1] recognized the ill-posedness of the Perona-Malik diffusion and proposed modifications to overcome the same. Since then, several nonlinear diffusion methods have been developed and a good account of these can be found in [5, 1, 8, 23, 31, 33]. All of these are nonlinear models and differ in the diffusivity coefficient and/or the diffusion term. Some of them are also supplemented with a reactive term. Another popular framework for image smoothing is the total variation or TV norm framework pioneered by Rudin et.al., [28] and further developed by Chan et.al., [6] and Strong and Chan [32]. The total variation methods yield nonlinear diffusion equations that are always derived from variational principles using the TV norm. In [20], Malladi and Sethian propose a unified approach to noise removal and image segmentation using the concept of min-max curvature flow. Based on the image data, a min/max switch was designed to select $min(\kappa, 0.0)$ or $max(\kappa, 0.0)$ so that the curvature based curve evolution smoothes out small oscillations, but maintains the essential properties of the shape. Results of implementation were shown on a variety of images yielding quality noise removal and image segmentation. In [31], Shah developed a common framework for curve evolution, image de-noising and segmentation, and anisotropic diffusion. In this work, a new segmentation functional was developed which lead to a coupled system of PDEs, one of them performed nonlinear smoothing of the input image and the other smoothed an "edge strength" function. Shah [31] demonstrated that all the existing curve evolution and anisotropic diffusion schemes reported in literature can be viewed as special cases of his method. In [9], Chen et. al., a nonlinear diffusion equation supplemented with reactive terms for achieving edge preserving smoothing was presented. *All of the methods discussed thus far are primarily applicable to the selective smoothing of scalar valued images*.

Smoothing vector valued images has been less popular than the scalar valued image data sets. In this context, Whitaker and Gerig introduced anisotropic vector-valued diffusion which was a direct extension of the work by Perona and Malik [25] to vector-valued images. The selective term in their work was based on the the gradient of the vector valued image, which is the Jacobian matrix. In [30] Sapiro et.al., introduced a selective smoothing technique where the selection term is not simply based on the gradient of the vector valued image. Instead, he showed that the stopping term should be a quantity related to the eigen values of the Riemanian metric tensor computed from the underlying surface defined by the vector valued image. They applied their selective smoothing technique to smooth noisy color images leading to impressive results. A very general flow called the Beltrami flow as a general framework for scalar and vector valued image smoothing was introduced in Kimmel et. al., [18] and it was shown that most flow-based smoothing schemes may be viewed as special cases in their framework. A generalization of the TV norm to handle vector-valued image smoothing was presented in Blomgren and Chan [3]. They showed that their generalization was natural and had desirable properties such as the rotational invariance in the image space etc. Existence and uniqueness of a solution to their evolution equation is yet to be explored but is not difficult to establish. There are many other PDE-based image smoothing techniques that we have not covered here but will refer the interested reader to a recent survey by Weickert [35] and also the special issue of the IEEE Transactions on Image Processing on PDE-based image processing [4].

Very briefly, we propose a novel and efficient weighted total variation (TV) norm based image smoothing scheme where in the raw image data (one image for each of the 7 directions) $\mathbf{S}$ is smoothed using a PDE which is obtained as a consequence of a *weighted TV norm minimization defined for vector valued functions*. The selective term in our work, is based on the eigen values of a diffusion tensor $\mathbf{D}$ that can be computed initially from the raw image data using the relationship $\mathbf{S} = S_0 exp- \sum_{ij} b_{ij} D_{ij}$, where, $\mathbf{S}$ is the vector of signal/image measurements taken along seven directions X, Y, Z, XY, YZ, XZ, XYZ, S_0 is a constant, b_{ij} is the magnetic field strength (which is a constant for a given direction) and D_{ij} are the entries of the $(3, 3)$ matrix representing the diffusion tensor measuring the diffusion of water inside the body being imaged. The selective term in this case $g(s) = 1/(1 + s)$ where $s = FA$ is the fractional anisotropy defined as [2] $FA = \frac{\sqrt{(\lambda_1 - \overline{\lambda})^2 + (\lambda_2 - \overline{\lambda})^2 + (\lambda_3 - \overline{\lambda})^2}}{\sqrt{\lambda_1^2 + \lambda_2^2 + \lambda_3^2}}$ where, λ_1, λ_3 and $\overline{\lambda}$ are the largest, smallest and average eigen values of the diffusion tensor D respectively. This selection criteria preserves the dominant anisotropic direction while smoothing the rest of the data. Another measure that works quite well is $s = (\lambda_1 - \lambda_3)/\lambda_3$. This selection criteria preserves the dominant anisotropic direction while smoothing the rest of the data. Note that since we are only interested in the fiber tracts which correspond to the streamlines of the dominant anisotropic direction, it is apt to choose such a selective

term as opposed to one that preserves edges in signal intensity as was done in [24].

1.1 Finding Stream Lines

Water in the brain preferentially diffuses along white matter fibers. By tracking the direction of fastest diffusion, as measured by MRI, non-invasive fiber tracking of the brain can be accomplished. Fibers tracks maybe constructed by repeatedly stepping in the direction of fastest diffusion. The direction along which the diffusion is dominant corresponds to the direction of eigen vector corresponding to the largest eigen value. In Conturo et. al., [11], fiber tracks were constructed by following the dominant eigenvector in 0.5 mm steps until a predefined measure of anisotropy fell below some threshold. This usually occurred in grey matter. The tensor, $\mathbf{D}$, was calculated at each step from interpolated DT-MRI data. This tracking scheme is primarily based on heuristics and is not grounded in well founded mathematical principles. Using methods well grounded in mathematical principles will allow us to better understand/quantify the strengths and weakness of the method/algorithm leading to a better overall performance.

In Mori et.al., [21] fiber tracking was achieved using several heuristics. The tracking algorithm starts from a voxel center and proceeds in the direction of the major axis of the diffusion ellipsoid. When the edge of the voxel is reached, the direction is changed to that of the neighboring voxel. Tracking stops when a measure of adjacent fiber alignment crosses a given threshold. One possible measure is the sum of inner products of nearby data points. This method was able to reconstruct well-known pathways through a rat brain. This method is also based on several data dependent heuristics for achieving the fiber tract mapping.

Given the dominant eigen vector field of the diffusion tensor in 3D, tracking the fibers (space curves) along this dominant eigen vector field is basically equivalent to finding the stream lines/integral curves in 3D of this vector field. Finding integral curves of vector fields is a well researched problem in the field of Fluid Mechanics [10]. The simplest solution would be to numerically integrate the given vector field using a stable numerical integration scheme such as a fourth order Runge-Kutta integrator [27]. However, this may not yield a regularized integral curve. In this paper, we pose the problem of finding stream lines of the dominant eigen vector field of the diffusion tensor in a variational framework incorporating smoothness constraints which regularize the integral curve. The variational principle formulation leads to a PDE which can be solved using efficient numerical techniques. We present the computed 3D fiber tracts produced for normal and injured spinal cords of rats using volume rendering techniques.

2 Image De-noising and Diffusion Tensor Computation

In this paper, we propose a novel technique for smoothing vector valued data that will be used in computing the diffusion tensor field and mapping out the fiber tracts. The novelty lies in the formulation that leads to a PDE which is different from the traditionally used PDEs in literature for vector valued image selective smoothing. The difference lies in both the selective term used as well as the fact that the PDE is derived from a minimization principle which does not involve arc length minimization as is used traditionally in most selective image smoothing schemes that are based on minimization principles. Note that there are several PDE-based schemes in literature that are not based on minimization principles [31, 34, 29, 20, 36].

Smoothing the raw vector valued image data is posed as a variational principle involving a first order smoothness constraint on the solution to the smoothing problem. Let $\hat{\mathbf{S}}(\mathbf{X})$ be the vector valued image that we want to smooth where, $\mathbf{X} = (x, y, z)$ and let $\mathbf{S}(X)$ be the unknown smooth approximation of the data that we want to estimate. We propose a weighted TV-norm minimization for smoothing the vector valued image $\mathbf{S}$. The variational principle for estimating a smooth $\mathbf{S}(\mathbf{X})$ is given by

$$\min_{\mathbf{S}} \mathcal{E}(\mathbf{X}) = \int_{\Omega} g(\lambda_+, \lambda_-) \sum_{i=1}^{7} \|\nabla S_i(\mathbf{X})\| + \mu/2 \sum_{i=1}^{7} \|S_i - \hat{S}_i\|^2 d\mathbf{X} \tag{1}$$

where, Ω is the image domain and μ is a regularization factor. The first term here is the regularization constraint on the solution to have a certain degree of smoothness and selective smoothing is achieved by the term $g(\lambda) = 1/[1 + \{(\lambda_+ - \lambda_-)/\lambda_+\}^2]$, where λ is the eigen value of the diffusion tensor computed from the initial data. This function has very small value (approaching zero) as the relative difference in the largest and smallest eigen values becomes large – stopping the smoothing at such locations – and vice versa. Since, the anisotropy in the image is well captured by the direction of the dominant eigen value, it is apt for us to preserve any discontinuities in the anisotropy while smoothing the data. Note that it is not the edges (local maxima in the gradient) in the DT image that we are interested in but its the anisotropy or the lack thereof that is crucial for the fiber tract mapping. The aforementioned selective smoothing criteria is therefore well justified and is also supported by the superior quality of the preliminary results (in comparison to the competing method described in [24]). The second term in the variational principle makes the solution faithful to the data to a certain degree. The parameter μ controls how close the smooth approximation should be to the

given data. The gradient descent of the above minimization is given by

$$\frac{\partial \mathrm{S}_i}{\partial t} = div\left(\frac{g(\lambda_+,\lambda_-)\nabla \mathrm{S}_i}{\|\nabla S_i\|}\right) - \mu(\mathrm{S}_i - \hat{\mathrm{S}}_i) \quad i = 1, ..., 7$$
$$\frac{\partial S_i}{\partial n}|_{\partial\Omega\times\Re^+} = 0 \ \ and \ \ \mathbf{S}(\mathbf{X}, t=0) = \hat{\mathbf{S}}(\mathbf{X}) \tag{2}$$

Note that this nonlinear PDE is different from the traditional nonlinear diffusion equations that are found in literature [31, 29, 20] which are curve evolution based schemes. The main difference is that there is NO $\|\nabla \mathrm{S}_i\|$ multiplicative factor in the first term on the right hand side. What difference does this make? Firstly, its asymptotic solution converges to the correct minimizer of 1 and the proof of convergence does not require the use of the viscosity methods as in [1]. Moreover, as in the traditional curve/surface evolution based nonlinear diffusion equations, if we include the aforementioned multiplicative factor $\|\nabla \mathrm{S}_i\|$, it is not clear if the asymptotic solution of the gradient descent equation 2 converges to the true minimizer of 1. The above variational principle is a generalization of the traditional TV-norm for the scalar valued functions but differs in obvious ways from the generalization presented in Blomgren and Chan [3]. The main difference being that we use a weighted TV-norm and our generalization does not have a square root and the square under the summation as in [3]. The existence and uniqueness questions for such a weighted TV-norm minimization have not been answered in literature to date. We present a sketch of this proof in the next section.

The above nonlinear PDE can be solved using efficient and stable numerical schemes. In this paper, we used an implicit method namely the Crank-Nicholson scheme [26]. It can also be solved using the lagged-diffusivity scheme discussed in [7] but we found the former to be more effective and stable.

2.1 Estimating the Stream Lines/Integral Curves

Once the diffusion tensor has been robustly estimated, the fiber tracts may be mapped by choosing seed points in the image lattice and using numerical integration techniques to determine the integral curves of the eigen vector field corresponding to the dominant eigen values. Several numerical integration schemes exist in literature [27]. The most widely used and stable numerical integration scheme for ordinary differential equations is the Runge-Kutta scheme of order four (RK4) [27]. The solution obtained by directly using the RK4 may not be at times desirable since there are no regularization constraints on the resulting integral curves/fibers which are space curves in this case. In order to have these space curves not exhibit very sharp twists and turns (e.g., those with corners), we can formulate the integral curve estimation problem as a variational principle. Thus, given the eigen vector field $\mathbf{v} = (v_1, v_2, v_3)^T$ corresponding to the dominant eigen values, our formulation of the variational principle involves minimizing the following functional:

$$\min_{\mathbf{c}} E(p) = \min_{\mathbf{c}} \int_0^1 |\mathbf{c}'(p)| + \frac{\beta}{2}|\mathbf{c}'(p) - \mathbf{v}(\mathbf{c}(p))|^2 dp \tag{3}$$

where, $\mathbf{c}(p) = (x(p), y(p), z(p))^T$, is the integral curve we want to estimate and $p \in [0, 1]$ is the parameterization of the curve, Ω is the domain over which the curves are to be determined and $\mathbf{v}(\mathbf{c}(p))$ is the vector field $\mathbf{v}$ restricted to the curve $\mathbf{c}(p)$. The first term in this functional $E(p)$ is seeking to minimize the L_1 norm of the first derivative of the curve i.e., seeking smooth curves and the second term requires that the tangent to the smooth curve that we seek be close to the the given dominant eigen vectors in an L_2 sense. The gradient descent i.e., the Euler-Lagrange expressed as an initial boundary value problem, of the variational principle in equation 3 is given by

$$\begin{aligned}\mathbf{c}_t =& |\mathbf{c}'(p)|k\mathbf{n} + \beta[\mathbf{c}''(p) - \mathbf{V}(\mathbf{c}(p))\mathbf{c}'(p)] + \\ & \beta\mathbf{V}^T(\mathbf{c}(p))(\mathbf{c}'(p) - \mathbf{v}(\mathbf{c}(p))\end{aligned} \tag{4}$$

where k is the curvature of the space curve, β is a regularization parameter and

$$\mathbf{V} = D\mathbf{v} = \begin{pmatrix} v_{1x} & v_{1y} & v_{1z} \\ v_{2x} & v_{2y} & v_{2z} \\ v_{3x} & v_{3y} & v_{3z} \end{pmatrix}$$

$\mathbf{V}^T$ = the transpose of $\mathbf{V}$. The curvature k is given by

$$k = \|\frac{d}{dp}\left(\frac{\mathbf{c}'(p)}{|\mathbf{c}'(p)|}\right)\|.$$

The above initial boundary value problem can be solved numerically using a variety of methods. We propose to use the Crank-Nicholson implicit method which is a very stable scheme (see [26]). Each iteration of this numerical iterative scheme requires the solution a sparse banded (tridiagonal and positive definite) linear system which can be solved in $O(n)$ time, where n is the size of the linear system equal to the number of discrete points on the space curve. As an initial condition for solving this PDE, we use the results obtained by simply integrating the given vector field numerically using a fourth order Runge-Kutta method [27]. The computed integral curves are superimposed on the original DTI data and visualized using a volume renderer. Results of this volume visualization are presented in section 4.

3 Existence and Uniqueness Results

In this section, we will briefly outline the approach for establishing the existence and uniqueness of a solution to the weighted TV-norm minimization equation 1. We will actually present the well-posedness result for a general weighted TV-norm minimization and our minimization problem (1), is included in this framework.

Consider the problem

$$\min_{u\in BV(\Omega,R^k)\cap L^2} E(u) = \min_{u\in BV(\Omega,R^k)\cap L^2} \int_\Omega \sum_{i=1}^{k} \{g|\nabla u_i| + \frac{1}{2}|u_i - I_i|^2\} \tag{5}$$

To study the well-posedness of this problem, it is necessary to introduce the concept of weighted TV norms for functions of bounded variation. Recalling definition of bounded variation (BV) spaces [15, 16].

Definition 1: Let $\Omega \subset R^n$ be an open set and let $f = (f_1, \ldots, f_k) \in L^1(\Omega, R^k)$. Define

$$\int_\Omega |\nabla f| = \sum_{i=1}^{k} \int_\Omega |\nabla f_i| =: \sum_{i=1}^{k} \sup_{\phi\in\Phi} \left\{ \int_\Omega f_i(x) div(\phi(x)) dx \right\}, \tag{6}$$

where

$$\Phi =: \{\phi = (\phi_1, \ldots, \phi_n) \in C_0^1(\Omega, R^n) |\ |\phi(x)| \le 1, \ for\ all\ x \in \Omega\}. \tag{7}$$

Definition 2: A function $f \in L^1(\Omega, R^k)$ is said to have bounded variation in Ω, if $\int_\Omega |\nabla f| < \infty$. We define $BV(\Omega, R^k)$ as the space of all functions in $L^1(\Omega, R^k)$ with bounded variation.

If $f \in BV(\Omega, R^k)$, ∇f_i $(i = 1, \ldots, k)$ then ∇f_i is an R^n valued Radon vector measure. This means

$$\int_\Omega f_i(x) div(\phi(x)) dx = -\int_\Omega \nabla f_i(x) \cdot \phi(x). \tag{8}$$

for all $\phi \in C_0^\infty(\Omega, R^n)$.

Definition 3: $f_m \in BV(\Omega, R^k)$ converges weakly in $BV(\Omega, R^k)$ to a function $f \in BV(\Omega, R^k)$, if for each $i = 1, \ldots, k$

$$\lim_{m\to\infty} \int_\Omega \phi \cdot \nabla f_{m_i} = \int_\Omega \phi \cdot \nabla f_i, \tag{9}$$

for all $\phi \in C_0^\infty(\Omega, R^n)$, where f_{m_i} is the i^{th} element of f_m.

Definition 4: Let $\Omega \subset R^n$ be an open set and $f = (f_1, \ldots, f_k) \in L^1(\Omega, R^k)$ and let g be continuous in Ω, with $\alpha_0 \le g \le \alpha_1$ for $x \in \Omega$, where α_0 and α_1 are positive constants. Define the weighted total variation norm of $f(x)$ with the weight function g, $\int_\Omega g|\nabla f|$ by

$$\begin{aligned} \int_\Omega g|\nabla f| &= \sum_{i=1}^{k} \int_\Omega g|\nabla f_i| \\ &=: \sum_{i=1}^{k} \sup_{\phi\in\Phi_g} \left\{ \int_\Omega f_i(x) div(\phi(x)) dx \right\}, \end{aligned} \tag{10}$$

where

$$\Phi_g =: \{\phi = 3D(\phi_1, \ldots, \phi_n) \in C_0^1(\Omega, R^n) | \ |\phi(x)| \le g, \ for\ all\ x \in \Omega\}.$$

Theorem 1 *Suppose that g satisfies all the assumptions in Definition 4 and $I \in L^2(\Omega, R^k)$. Then, the minimization problem (5) has a unique solution $u \in BV(\Omega, R^n) \cap L^2$.*

Proof Outline 1 *The uniqueness of the minimum in (5) follows by the strict convexity of the functional*

$$\int_\Omega \sum \left\{ g\|\nabla u_i\| + (1/2)\|u_i - I_i\|^2 \right\}. \tag{11}$$

(The second term is strictly convex). The existence is proved as follows: Let u_n be a minimizing sequence. Then u_n is bounded in L^2 because of the second term in (5). Using the convexity of the functional, we may assume that u_n converges in L^2 to say u. Then, we use the lower semi-continuity of the norm is BV spaces to conclude that u is a minimizer.

In order to use the gradient descent method for solving (5), we consider the following evolution problem:

$$\partial_t u_i = div(g(\nabla u_i/|\nabla u_i|)) - (u_i - I_i),\ x \in \Omega,\ t > 0 \tag{12}$$

$$u_i(x, 0) = I_i(x), \ \ x \in \Omega, \ \ \frac{\partial u_i}{\partial n} = 0, \ \ x \in \partial\Omega,\ t \ge 0, \tag{13}$$

where $i = 1, \ldots, k$, and n is the outward unit norm to Ω.

Definition 4: A function $u = (u_1, \ldots, u_k) \in L^2(0, T; BV(\Omega, R^k) \cap L^2)$ is called a weak solution of (12)-(13), if for each $i = 1, \ldots, k$ $\partial_t u_i \in L^2(0, T; L^2(\Omega))$, $u_i = I_i$, a.e. in Ω, and u_i satisfies

$$\begin{aligned} &\int_0^s \int_\Omega \partial_t u_i (v_i - u_i) + \int_0^s \int_\Omega g|\nabla v_i| \\ &- \int_0^s \int_\Omega (u_i - I_i)(v_i - u_i) \ge \int_0^s \int_\Omega g|\nabla u_i|, \end{aligned} \tag{14}$$

for $a.e.\ s \in [0, T]$, $all\ v = (v_1, \ldots, v_k) \in L^2(0, T; BV(\Omega, R^k) \cap L^2)$. We can now prove the following theorem.

Theorem 2 *The problem (12)-(13) has an unique solution $u \in L^2(0,T;BV(\Omega,R^k)) \cap L^\infty$ in the sense of (14). Moreover, as $t \to \infty$ $u(\cdot,t)$ converges weakly in $BV(\Omega,R^k) \cap L^2$ to a function u_∞, which solves (5).*

Proof Outline 2

$$\partial_t u_i = div\left(g(\nabla u_i)^{(p-2)}\nabla u_i\right) - (u_i - I_i)$$

The existence here is well known. We show that the solution u_p is indeed in L^∞. We obtain uniform estimates of the norms to show that the limit as $p \to 1$ of the asymptotic limits $u_p \to \infty$ exists and is indeed a minimizer i.e., a solution in BV of (5).

4 Experimental Results

In this section, we present two sets of experiments on, application of the proposed selective smoothing to the raw image data yielding smoothed tensor fields, and the computed fiber tract maps from these smoothed data for the case of a normal and an injured rat spinal cord respectively.

In both the experiments, we first smooth the seven 3D directional images using the novel selective smoothing technique outlined in section 2. Following this, the diffusion tensor is estimated from the smoothed data using a standard least squares technique. The fractional anisotropy, the color trace of the diffusion tensor (sum of the diagonal terms of the diffusion tensor in an RGB color space), the dominant eigen value as well as the color map of the direction cosines of the eigen vector corresponding to the dominant eigen value are computed. The latter color map depicts the standard axis (X,Y,Z) toward which direction of diffusion in the data is dominant and the dominant eigen value corresponds to the magnitude of this dominant diffusion direction. *Red corresponding to the X component, Green for the Y component and Blue for the Z component*. This color coding will indicate the standard direction (X, Y or Z) along which the dominant eigen vector has the strongest component. Images obtained as a result of these computations from raw data, smoothed data using a competing smoothing method outlined in Parker et.al., [24] and smoothed data using our proposed method are depicted for the two data sets. In addition, estimated fiber tracts from the smoothed data using the proposed fiber tract/integral curves computation scheme are also depicted for the data sets. The results of smoothing for the two examples are shown in Figures 1 and 3 which are organized as follows: first row contains images computed from raw (noisy) data, second row contains images computed using methods in [24] and third row contains computed images using the proposed image smoothing technique. Note the superior performance of the proposed smoothing scheme in comparison to the method in Parker et .al., [24].

Figure 2 depicts the computed 3D fiber tracts for a normal rat spine and is organized as follows: On the top left, computed fiber tracts are shown in green. These fiber tracts are supposed to run along the length of the spinal cord in the white matter which is exactly what our computations reveal. The top right image depicts a volume rendered DT-MR data set with the fiber tracts overlayed in green. The bottom row shows two different cut away views of the overlayed fiber tracts on the volume rendered DT-MR scan of this normal rat spinal cord.

Figure 3, depicts the results obtained from an injured rat spine by application of the proposed smoothing in comparison to results obtained from raw data and the competing method in [24]. Fiber tract mapping is also shown for this injured spine in figure 4. These results are organized as in the figures 1 and 2. As evident, the injury has caused a large cavity down the length of the spine and there are no fibers in this region. Also evident is the fact that our data smoothing results are superior to smoothing performed by the Perona and Malik scheme [25] which was used in [24]. Also, the visual quality of the fiber tracts is satisfactory.

In the above presented results, what is to be noted is that we have demonstrated a proof of concept for the proposed data smoothing and fiber tract mapping algorithms in the case of the normal and injured rat spinal cords respectively. The quality of results obtained is reasonably satisfactory for visual inspection purposes but quantitative validation needs to be performed and will be the focus of our future efforts.

5 Conclusions

In this paper, we presented a new weighted TV-norm minimization formulation for smoothing vector-valued data specifically tuned to computation of smooth diffusion tensor MR images. Existence and uniqueness of a solution for the weighted TV-norm minimization is outlined. The smoothed vector valued data was then used to compute a diffusion tensor image using standard least squares technique. Fiber tracts in 3D were computed as the integral curves of the dominant eigen vector field obtained from the diffusion tensor image. The integral curve computation was formulated in a variational framework as well and solved using efficient numerical schemes. Finally, results of fiber tract mapping of a normal and an injured rat spinal cord were depicted using standard volume rendering techniques. The computed fiber tracts are quite accurate when inspected visually. However, quantitative validation of the computed fiber tracts is essential and will be the focus of our future efforts.

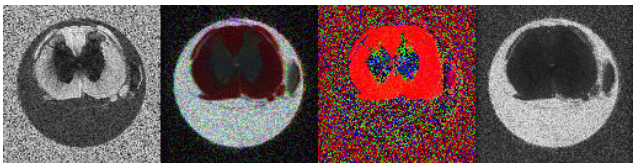

(a)

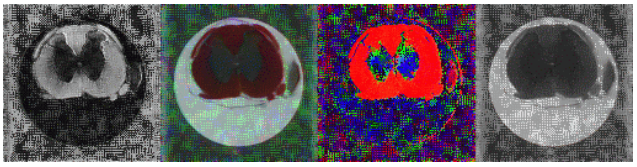

(b)

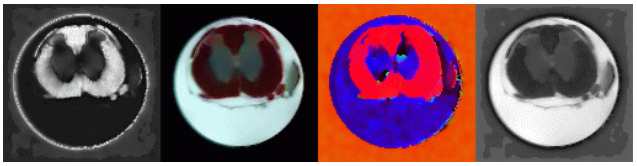

(c)

Figure 1: Normal Cord, left to right: FA, Color Trace, direction cosines of the dominant eigen vector, and the dominant eigen value. First row: results computed from raw data, Row-2: results computed using Perona-Malik diffusion, Row-3: results from the proposed smoothing.

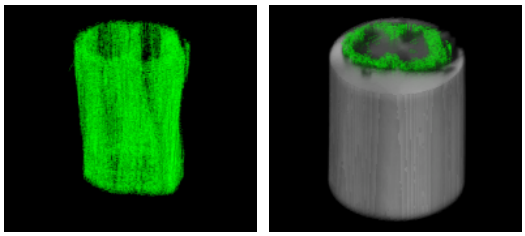

(a) (b)

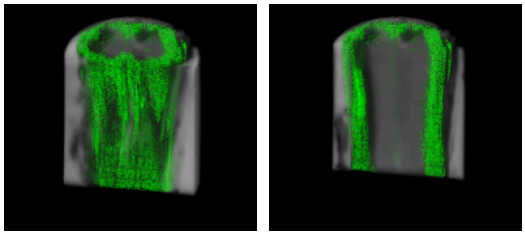

(c) (d)

Figure 2: Normal rat spinal cord: computed fibers overlayed on volume rendered DT-MR data and its cut away views.

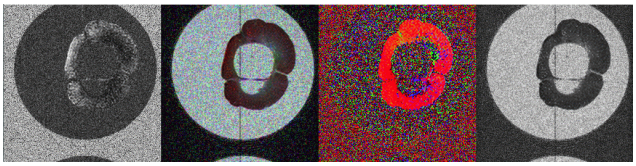

(a)

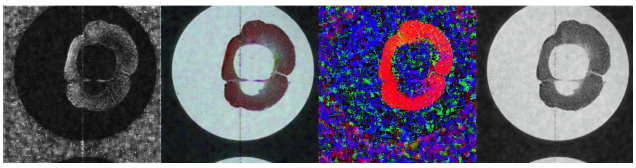

(b)

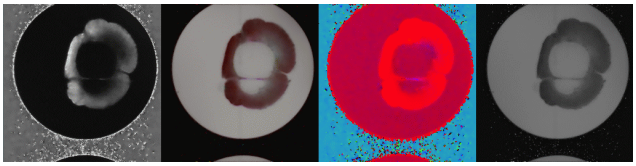

(c)

Figure 3: Injured Cord, left to right: FA, Color Trace, direction cosines of the dominant eigen vector and the dominant eigen value. First row: results computed from raw data, Row-2: results computed using Perona-Malik Diffusion, Row-3: results from the proposed smoothing.

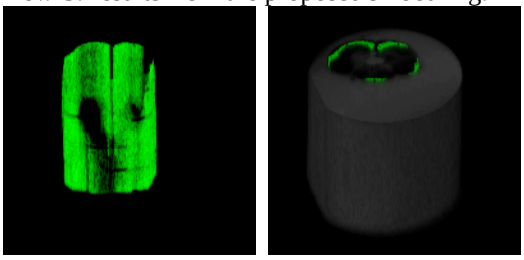

(a) (b)

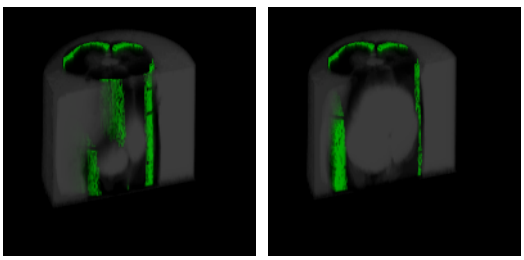

(c) (d)

Figure 4: Injured rat spinal cord: computed fibers overlayed on volume rendered DT-MR data and its cut away views.

References

[1] L.Alvarez, P. L. Lions, and J. M. Morel, "Image selective smoothing and edge detection by nonlinear diffusion. ii," *SIAM J. Numer. Anal.*, vol. 29, no. 3, pp. 845–866, June 1992.

[2] P. J. Basser and C. Pierpaoli "Microstructural and Physiological Features of Tissue Elucidated by Quantitative-Diffusion-Tensor MRI" J. Magn. Reson. B 110, 209-219 (1996)

[3] P. Blomgren and T. F. Chan,"Color TV: Total Variation Methods for Restration of Vector-Valued Images," *IEEE Transaction on Image Processing*, Vol. 7, no. 3, pp. 304-309, March, 1998.

[4] V. Caselles, J. M. Morel, G. Sapiro and A. Tannenbaum,*IEEE Trans. on Image Processing*, special issue on PDEs and geometry-driven diffusion in image processing and analysis, Vol 7, No. 3, 1998.

[5] F.Catte, P.L. Lions, J.M. Morel, and T.Coll, "Image selective smoothing and edge detection by nonlinear diffusion," *SIAM Journal of Numerical Analysis*, vol. 29, pp. 182–193, 1992.

[6] T. F. Chan, G. Golub, and P. Mulet, "A nonlinear primal-dual method for TV-based image restoration," in *Proc. 12th Int. Conf. Analysis and Optimization of Systems: Images, Wavelets, and PDE's*, Paris, France, June 26-28, 1996, M. Berger et al., Eds., no. 219, pp. 241-252.

[7] T. Chan and P. Mulet, "On the Convergence of the Lagged Diffusivity Fixed Point Method in Total Variation Image Restoration," September 1997, CAM TR-97-46.

[8] P.Charbonnier, L.Blanc-Feraud, G.Aubert, and M.Barlaud, "Two deterministic half-quadratic regularization algorithms for computed imaging,," in in *Proc. of the IEEE Intl. Conf. on Image Processing* (ICIP), 1994, vol. 2, pp. 168–172, IEEE Computer Society Press.

[9] Y. Chen, B. C. Vemuri and L. Wang,"Image denoising and segmentation via nonlinear diffusion," *Computers and Mathematics with Applications*, Vol. 39, No. 5/6, 2000, pp. 131-149.

[10] A. Chorin, *Computational Fluid Mechanics, Selected papers*, Academic Press, 1989.

[11] T. E. Conturo, R. C. McKinstry, E. Akbudak, and B. H. Robinson "Encoding of Anisotropic Diffusion with Tetrahedral Gradients: A General Mathematical Diffusion Formalism and Experimental Results" Magn. Reson. Med. 35, 399-412 (1996)

[12] T. E. Conturo, N. F. Lori, T. S. Cull, E. Akbudak, A. Z. Snyder, J. S. Shimony, R. C. McKinstry, H. Burton and M. E. Raichle "Tracking neuronal fiber pathways in the living human brain" Proc. Natl. Acad. Sci. USA 96, 10422-10427 (1999)

[13] F. Crick and E. Jones "Backwardness of human neuroanatomy" Nature 361, 109-110 (1993)

[14] P. Douek, R. Turner, J. Pekar, N. Patronas and D. LeBihan "MR color mapping of myelin fiber orientation" J. Comput. Assist. Tomogr. 15, 923-929 (1991)

[15] L.C.Evans and R.Gariepy, "Measure theory and fine properties of functions", Studies in Advanced Mathematics, 1992.

[16] E. Giusti, "Minimal surfaces and functions of bounded variation", Birkhauser, Basel, 1985.

[17] D. K. Jones, A. Simmons, S. C. R. Williams and M. A. Horsfield, "Non-invasive assessment of axonal fiber connectivity in the human brain via diffusion tensor MRI" *Magn. Reson. Med.*, 42, 37-41 (1999).

[18] R.Kimmel, N.Sochen, and R.Malladi, "Images as embedding maps and minimal surfaces:movies, color and volumetric medical images,," in *Proc. of the IEEE Conf. on Computer Vision and Pattern Recognition*, June 1997, pp. 350–355.

[19] N. Makris, A. J. Worth, A. G. Sorensen, G. M. Papadimitriou, O. Wu, T. G. Reese, V. J. Wedeen, T. L. Davis, J. W. Stages, V. S. Caviness, E. Kaplan, B. R. Rosen, D. N; Pandya, and D. N. Kennedy "Morphometry of in vivo human white matter association pathways with diffusion-weighted magnetic resonance imaging," *Ann. Neurol.*, 42, 951-962 (1999).

[20] R.Malladi and J.A. Sethian, "A unified approach to noise removal, image enhancement and shape recovery," *IEEE Trans. on Image Processing*, vol. 5, no. 11, pp. 1554–1568, 1996.

[21] S. Mori, B. J. Crain, V. P. Chacko and P. C. M. van Zijl "Three-dimensional tracking of axonal projections in the brain by magnetic resonance imaging" *Ann. Neurol.*, 45, 265-269 (1999)

[22] M.Nitzberg and T.Shiota, "Nonlinear image filtering with edge and corner enhancement,," *IEEE Transactions on Pattern Analysis and Machine Intelligence*, vol. 14, no. 8, pp. 826–832, 1992.

[23] P.J. Olver, G.Sapiro, and A.Tannenbaum, "Invariant geometric evolutions of surfaces and volumetric smoothing," *SIAM J. Appl. Math.*, vol. 57, pp. 176–194, 1997.

[24] G.J. M. Parker, J. A. Schnabel, M. R. Symms, D. J. Werring and G. J. Baker, "Nonlinaer smoothing for reduction of systematic and randome errors in diffusion tensor imaging," *Magn. Reson. Imag.*, 11, 702-710, 2000.

[25] P.Perona and J.Malik, "Scale-space and edge detection using anisotropic diffusion," *IEEE Trans. PAMI*, vol. 12, no. 7, pp. 629–639, 1990.

[26] L. Lapidus and G. F. Pinder, *Numerical solution of partial differential equations in science and engineering*, John Wiley and Sons, 1982.

[27] W.H.Press, B.P.Flannery, S.A.Teukolsky and W.T.Vetterling, [1992], *Numerical Recipes in C: The Art of Scientific Computing*. Cambridge University Press, Cambridge, England, second edition.

[28] L. I. Rudin, S. Osher, and E. Fatemi, "Nonlinear variation based noise removal algorithms", Physica D, vol. 60, pp. 259-268, 1992.

[29] G.Sapiro, "Vector-valued active contours," in *IEEE Proc. of the CVPR*. 1996, pp. 680–685, IEEE Computer Soc. Press.

[30] G.Sapiro and D.L. Ringach, "Anisotropic diffusion of multivalued images with applications to color filtering," *IEEE Trans. on Image Processing*, vol. 5, pp. 1582–1586, 1996.

[31] J.Shah, "A common framework for curve evolution, segmentation and anisotropic diffusion," in *IEEE Conf. on Computer Vision and Pattern Recognition*, 1996.

[32] D. M. Strong and T. F. Chan, "Relation of regularization parameter and scale in total variation based denoising," in Proc. IEEE Workshop on Mathematical Methods in Biomedical Image Analysis, 1996

[33] J.Weickert, "A review of nonlinear diffusion filtering,," in *Scale-space theory in computer vision,*, (Eds.) B. ter Haar Romney, L.Florack, J. Koenderink, and M. Viergever, Eds. 1997, vol. 1252, of *Lecture Notes in Computer Science,*, pp. 3–28, Springer-Verlag.

[34] R. Whitaker and G. Gerig, "Vector-valued diffusions," in *Geometry-driven Diffusions in Computer Vision*, B. Romney et.al., (Eds.), Kluwer, 1994.

[35] J.Weickert, "A review of nonlinear diffusion filtering,," in *Scale-space theory in computer vision,*, (Eds.) B. ter Haar Romney, L.Florack, J. Koenderink, and M. Viergever, Eds. 1997, vol. 1252, of *Lecture Notes in Computer Science,*, pp. 3–28, Springer-Verlag.

[36] A. Yezzi, Jr.,"Modified Curvature Motion for Image Smoothing and Enhancement," *IEEE Transaction on Image Processing*, Vol. 7, no. 3, pp. 345-352, March, 1998.

[37] W. Young "Secondary injury mechanisms in acute spinal cord injury" J. Emerg. Med. 13, 13-22 (1993)